

# Surface wettability and contact angle analysis by dissipative particle dynamics

Tzung-Han Lin<sup>1</sup>, Wen-Pin Shih<sup>1</sup> and Chuin-Shan Chen<sup>\*2</sup>

<sup>1</sup>*Department of Mechanical Engineering, National Taiwan University, Taipei, Taiwan*

<sup>2</sup>*Department of Civil Engineering, National Taiwan University, Taipei, Taiwan*

*(Received November 15, 2012, Revised November 26, 2012, Accepted December 7, 2012)*

**Abstract.** A dissipative particle dynamics (DPD) simulation was presented to analyze surface wettability and contact angles of a droplet on a solid platform. The many-body DPD, capable of modeling vapor-liquid coexistence, was used to resolve the vapor-liquid interface of a droplet. We found a constant density inside a droplet with a transition along the droplet boundary where the density decreased rapidly. The contact angle of a droplet was extracted from the isosurfaces of the density generated by the marching cube and a spline interpolation of 2D cutting planes of the isosurfaces. A wide range of contact angles from 55° to 165° predicted by the normalized parameter ( $|A_{SL}|/B_{SL}$ ) were reported. Droplet with the parameters  $|A_{SL}| > 5.84B_{SL}^{0.297}$  was found to be hydrophilic. If  $|A_{SL}|$  was much smaller than  $5.84B_{SL}^{0.297}$ , the droplet was found to be superhydrophobic.

**Keywords:** dissipative particle dynamics; contact angle; surface wettability; hydrophilic; hydrophobic.

---

## 1. Introduction

Surface wettability is an important phenomenon for the development of microfluidic systems and biocompatible materials. Surface energy on the solid, liquid and vapor interfaces is paramount to surface wettability (Adamson 1997). Meanwhile, surface roughness and morphology also play an important role on the phenomenon (Bico *et al.* 1999, He *et al.* 2003). Surface wettability can be characterized by the contact angle of a droplet. In this study, many-body dissipative particle dynamics (DPD) that is capable of resolving vapor-liquid coexistence through the density variance will be used to analyze contact angles of a droplet on a solid platform.

The DPD method was introduced by Hoogerbrugge and Koelman (1992) as a “cheap” way to study thermodynamic and hydrodynamic behavior at mesoscopic length and time scales (Frenkel and Smit 2002). Different from molecular dynamics (MD) (Allen and Tildesley 1989, Chen *et al.* 2008, Zhao and Aluru 2008), DPD integrates out the fast motion of atoms into additional dissipative and random forces. Espanol and Warren (1995) provided a proper statistical-mechanical basis for DPD. They derived the stochastic differential equations and Fokker-Planck equations and showed that the dissipative and random forces in DPD are correlated for the system to follow a constant

---

\* Corresponding author, Professor, E-mail: [dchen@ntu.edu.tw](mailto:dchen@ntu.edu.tw)

temperature ensemble. DPD time integration scheme follows closely with those used in MD (Allen and Tildesley 1989). Groot and Warren (1997) introduced a modified velocity-Verlet algorithm for integrating the equations of motion in DPD. They showed that the integration efficiency of the modified velocity-Verlet algorithm is about 50 times of the Euler algorithm.

Surface wettability involves vapor-liquid-solid interfacial behavior with mesoscopic length and time scales. The subject is suitable for DPD simulation but it has received a very limited attention. Jones *et al.* (1999) used a many-body DPD simulation to study contact angle hysteresis on the liquid-solid interface and did not take the vapor-liquid interface into consideration. Recently, Warren (2003) proposed a many-body DPD for vapor-liquid coexistence. The vapor-liquid interface is coexistent and can be determined from the variance of local density of liquid particles. In this study, we focus on using many-body DPD advanced by Warren (2003) to study surface wettability phenomenon. In particular, feasible DPD parameters for predicting contact angles of a droplet are investigated.

## 2. DPD model

DPD is a particle-based simulation. In DPD, the total force on a particle  $i$  consists of a conservative force ( $\mathbf{F}_{ij}^C$ ), a random force ( $\mathbf{F}_{ij}^R$ ) and a dissipative force ( $\mathbf{F}_{ij}^D$ )

$$\mathbf{f}_i = \sum_{j \neq i} \mathbf{F}_{ij} = \sum_{j \neq i} (\mathbf{F}_{ij}^C + \mathbf{F}_{ij}^R + \mathbf{F}_{ij}^D) \quad (1)$$

where  $\mathbf{F}_{ij}$  is a pair force exerted on the particle  $i$  due to the interaction from a neighboring particle  $j$ . The conservative force ( $\mathbf{F}_{ij}^C$ ) contains the soft interaction between particles

$$\mathbf{F}_{ij}^C = Aw_C(r_{ij})\mathbf{e}_{ij} + B(\rho_i + \rho_j)w_{CD}(r_{ij})\mathbf{e}_{ij} \quad (2)$$

$$w_C(r_{ij}) = \begin{cases} (1 - r_{ij}/r_c) & \text{if } r_{ij} < r_c \\ 0 & \text{otherwise} \end{cases} \quad (3)$$

$$w_{CD}(r_{ij}) = \begin{cases} (1 - r_{ij}/r_d) & \text{if } r_{ij} < r_d \\ 0 & \text{otherwise} \end{cases} \quad (4)$$

$$\rho_i = \frac{15}{2\pi r_d^2} \sum_j (1 - r_{ij}/r_d)^2, \quad \text{for } r_{ij} < r_d \quad (5)$$

in which  $r_{ij}$  is the distance between particles  $i$  and  $j$ ,  $\mathbf{e}_{ij}$  is the corresponding unit vector,  $\mathbf{e}_{ij} = (\mathbf{r}_i - \mathbf{r}_j)/|r_{ij}|$  and  $\rho_i$  and  $\rho_j$  are the density of the particles  $i$  and  $j$ , respectively. The magnitude of the conservative force depends on the positions of neighboring particles. The factors  $A$  and  $B$  are used for tuning the maximum amplitudes for attractive and repulsive forces, respectively. A shorter cutoff range  $r_d$ , which is less than the main cutoff  $r_c$ , is used for tuning the cutoff range of the repulsive force. It should be noted that the conservative force in a conventional DPD only has a repulsive term. Different from the conventional DPD, the conservative force in Warren (2003) consists of the attractive and repulsive terms in order to model liquid-vapor coexistence. In addition, particles' local densities are introduced in the repulsive term.

The random force,  $\mathbf{F}_{ij}^R$ , is introduced in DPD to capture thermal fluctuations from Brownian motion

$$\mathbf{F}_{ij}^R = \sigma w_R(r_{ij}) \xi_{ij} \Delta t^{-1/2} \mathbf{e}_{ij} \quad (6)$$

in which  $\xi_{ij}$  is a random variable with Gaussian distribution. It has a zero mean, unit variance and  $\xi_{ij} = \xi_{ji}$ . The  $\sigma$  is a thermostat coefficient. The dissipative force,  $\mathbf{F}_{ij}^D$ , is introduced in DPD to capture the viscous effect of the particle motion

$$\mathbf{F}_{ij}^D = -\gamma w_D(r_{ij}) (\mathbf{v}_{ij} \cdot \mathbf{e}_{ij}) \mathbf{e}_{ij} \quad (7)$$

$$\sigma^2 = 2\gamma k_B T \quad (8)$$

$$w_D(r_{ij}) = [w_R(r_{ij})]^2 \quad (9)$$

The dissipative force depends on the relative velocity  $\mathbf{v}_{ij}$  between particles  $i$  and  $j$ ,  $\mathbf{v}_{ij} = \mathbf{v}_i - \mathbf{v}_j$  in which  $\mathbf{v}_i$  and  $\mathbf{v}_j$  denote the velocities of particles  $i$  and  $j$ , respectively.  $\gamma$  is the coefficient for the dissipative force. The fluctuation-dissipation theorem is used in Eqs. (8) and (9) to correlate the coefficients and weighing functions in the random and dissipative forces where  $k_B$  is the Boltzmann's constant and  $T$  is temperature in DPD unit (Español and Warren 1995).

The DPD particles are driven by the conservative, random and dissipative forces and move incrementally based on Newton's second law. A modified velocity-Verlet algorithm is often used for numerical time integration (Groot and Warren 1997)

$$\begin{aligned} \mathbf{r}_i(t + \Delta t) &= \mathbf{r}_i(t) + \mathbf{v}_i(t)\Delta t + \mathbf{f}_i(t) \cdot (\Delta t)^2/2 \\ \tilde{\mathbf{v}}_i(t + \Delta t) &= \mathbf{v}_i(t) + \mathbf{f}_i(t)\Delta t/2 \\ \mathbf{f}_i(t + \Delta t) &= \mathbf{f}_i(\mathbf{r}_i(t + \Delta t), \tilde{\mathbf{v}}_i(t + \Delta t)) \\ \mathbf{v}_i(t + \Delta t) &= \mathbf{v}_i(t) + (\mathbf{f}_i(t) + \mathbf{f}_i(t + \Delta t))\Delta t/2 \end{aligned} \quad (10)$$

The algorithm is adapted herein to resolve the motion of particles.

### 3. Surface wettability simulation

Numerical models with a droplet on a solid platform were designed to model the surface wettability. The contact angle of the simulated droplet was extracted. Initially, a solid cube was constructed with  $20 \times 20 \times 2$  in length, width and height in the DPD unit, respectively. A droplet hemisphere was constructed with 12 DPD-unit in diameter as shown in Fig. 1. The particles were ordered initially as face centered cubic (FCC) with a unit length to fill up the solid cube and droplet hemisphere. The solid particles in the solid cube were freezing, and the liquid particles in the droplet were movable subjected to Eq. (1). About 15,000 and 20,000 particles were used in the droplet and solid cube regions, respectively. Because the solid particles were freezing, all the interactions among solid-solid particles were discarded and their attractive and repulsive parameters  $A_{SS}$  and  $B_{SS}$  were set to be zero. The attractive and repulsive parameters for liquid-liquid interaction were denoted as  $A_{LL}$  and  $B_{LL}$ . The values and other parameters listed in Table 1 were taken directly from Warren (2003). These parameters were capable for the droplet to resolve the liquid-vapor interface. The parameters for the liquid-solid interaction were denoted as  $A_{SL}$  and  $B_{SL}$  to manipulate

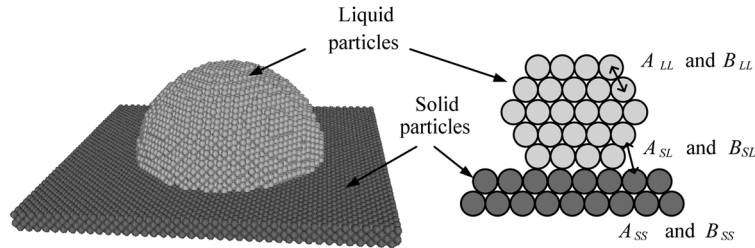


Fig. 1 A droplet on a solid platform is simulated with two kinds of DPD particles

Table 1 Simulation parameters on liquid-liquid interface

Mean of liquid density	$\langle \rho_l \rangle$	5.8
Short range for repulsive force	$r_d$	0.75*
Cutoff distance	$r_c$	1.0*
Liquid-liquid attraction amplitude	$A_{LL}$	-40*
Liquid-liquid repulsion amplitude	$B_{LL}$	25*
Coefficient for random force	$\sigma$	7.45*
Coefficient for dissipative force	$\gamma$	27.75125*
Time step	$\Delta t$	0.009

\*These parameters have been used in Warren (2003) to model the liquid-vapor co-existent state

the surface wettability phenomenon.

Because the simulation for reaching the steady state was time consuming, we set the liquid particle cluster as a hemisphere to shorten the simulation time. Both hemisphere-shaped and sphere-shaped droplet clusters had been used in DPD simulation and no notable effects were found for the steady-state solutions. A proper time increment for DPD simulation could be obtained from the balance between a global density ( $\bar{\rho}$ ) and the mean of local densities. We set a measuring box with the width of 2 inside the droplet and above the solid platform to monitor the global and local densities. The global density  $\bar{\rho}$  was obtained by counting the numbers of particles inside the box and the mean of the local densities was obtained from Eq. (5). We took the average of global densities at the first 200 integration steps and compared it with the mean of local densities. The results shown in Fig. 2 indicated that a suitable time increment for our DPD simulation was about 0.009.

#### 4. Results and discussion

Contact angles of a droplet are used to characterize surface wettability. If the contact angle is greater than 90 degrees, the surface is hydrophobic. If the contact angle is lesser than 90 degrees, the surface is hydrophilic. In our DPD simulation, liquid particles started aggregating and showed an assembling tendency. The contact angle of the droplet was determined from the steady-state solutions (Fig. 3). In the hydrophobic case, the liquid particles bounced, and then stitched on the solid plate. The system reached the steady state quickly. In the hydrophilic case, the liquid particles

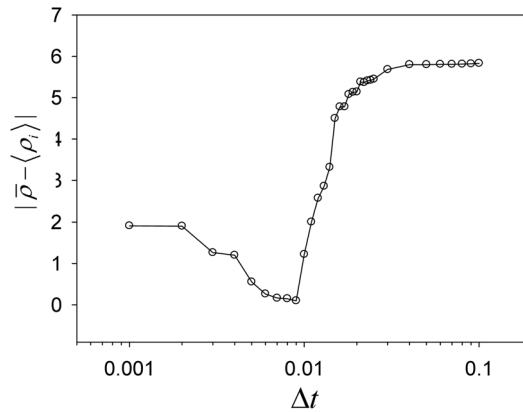


Fig. 2 Determination of the time increment for integration by calculating the difference between global and local densities

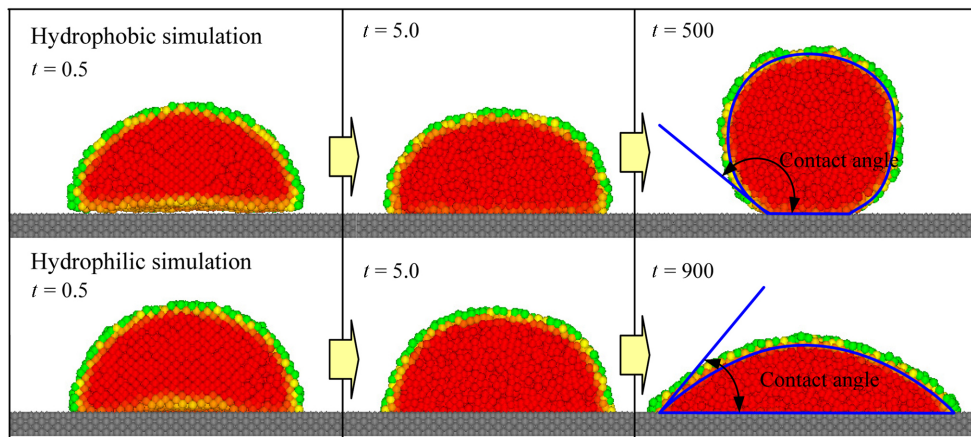


Fig. 3 The color intensities indicate variant densities on the cross sections of droplets. Top row illustrates simulation for a hydrophobic droplet with  $A_{SL} = -5$  and  $B_{SL} = 20$ . Bottom row illustrates a hydrophilic droplet with  $A_{SL} = -20$  and  $B_{SL} = 20$ . The transition zone of densities is used to determine the contact angle (right column)

near the solid plate started wriggling and reached the steady state slowly.

Inside the droplet, there was a quasi-uniform region with a constant density, followed by a transition zone where the density decreased rapidly. In our simulation, once the local density of the liquid particles was small enough,  $\rho_i \cong 1$ , the particle was considered as in the vapor phase. A marching cube method (Lorenzen and Cline 1987) was developed to smooth the field of local densities from the particles and to resolve the transition zone. Each density of liquid particles was re-allocated to its neighboring grids according to linear interpolation in the three orthogonal directions. Consequently, each grid had partial densities from its neighboring liquid particles. The precise interpolation for the isosurfaces was carried out. A threshold  $\rho_c$  equal to 1 was assigned for the marching cube to determine the liquid-vapor interface. Fig. 4 shows two examples from the hydrophobic and hydrophilic results. Once the isosurfaces were determined, the volume and mean density of a droplet were readily found.

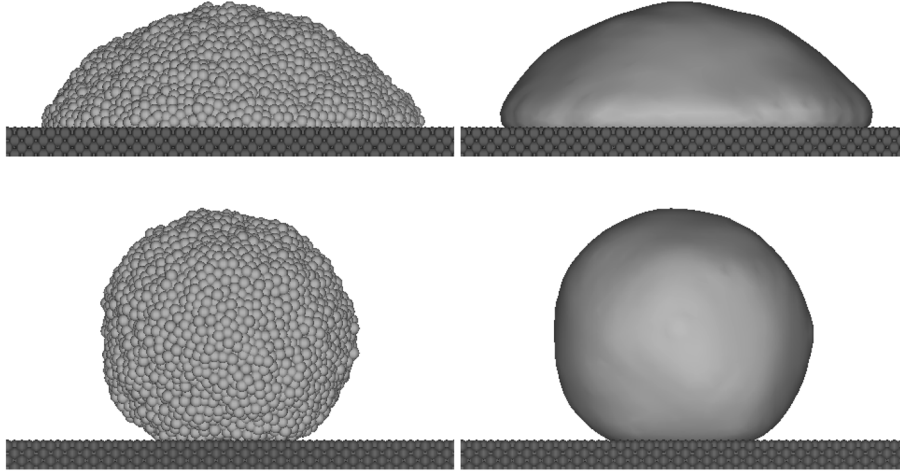


Fig. 4 The transitional profiles of densities are represented by the isosurfaces. The isosurfaces are determined by the marching cube by setting  $\rho = 1$

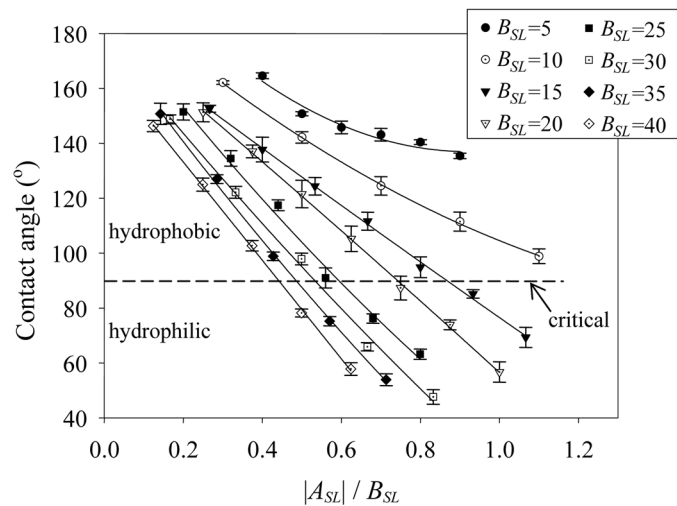


Fig. 5 Predicted contact angle versus the normalized parameter  $|A_{SL}|/B_{SL}$

In order to measure the contact angle of a 3D droplet, 2D cutting planes from the isosurfaces were performed. The 1D vapor-liquid interfacial profile in a 2D cutting plane was obtained by fitting a spline with five manually specified points along the transition zone. The contact angle was the inclined angle between a tangent line and a base line, which were formed by liquid-vapor and liquid-solid interfaces, respectively. The contact angles were sampled by at least fifty times for each simulation. Typically, a normal distribution was obtained from these results and the mean and variance were used to characterize the predicted contact angles from DPD simulation.

The hydrophobic and hydrophilic phenomena can be controlled by the attractive and repulsive parameters between liquid and solid particles ( $A_{SL}$  and  $B_{SL}$ ). Fig. 5 plots the mean and variance of the predicted contact angles versus the normalized parameter ( $|A_{SL}|/B_{SL}$ ). We note that the contact

angle and the normalized parameter have an approximately linear relation for  $B_{SL} > 10$ . The transition from hydrophobic to hydrophilic can be furthermore determined from interpolation of these results. Droplet with the parameters  $|A_{SL}| > 5.84B_{SL}^{0.297}$  was found to be hydrophilic. If  $|A_{SL}|$  was much smaller than  $5.84B_{SL}^{0.297}$ , the droplet was found to be superhydrophobic.

## 5. Conclusions

DPD simulation was used to characterize vapor-liquid-solid interfacial evolutions. Contact angles of a droplet were resolved from marching cube and spline interpolation of density variation. A wide range of contact angles from  $55^\circ$  to  $165^\circ$  predicted by the normalized parameter ( $|A_{SL}|/B_{SL}$ ) were reported. Droplet with the parameters  $|A_{SL}| > 5.84B_{SL}^{0.297}$  was found to be hydrophilic. If  $|A_{SL}|$  was much smaller than  $5.84B_{SL}^{0.297}$ , the droplet was found to be superhydrophobic.

## Acknowledgements

Computational resources were provided by the National Center for High-performance Computing and National Taiwan University. CSC would like to acknowledge funding supported by National Science Council of Taiwan (NSC 100-2628-E-002-035-MY3, NSC 100-2628-E-002-004, NSC 100-2627-E-002-001) and National Taiwan University (10R80920-05).

## References

- Adamson, A.W. (1997), *Physical chemistry of surfaces*, 6th ed., John Wiley & Sons, New York.
- Allen, M.P. and Tildesley, D.J. (1989), *Computer simulation of liquids*, Clarendon Press.
- Bico, J., Marzolin, C. and Quere, D. (1999), "Pearl drops", *Europhys. Lett.*, **47**(2), 220.
- Chen, C.S., Wang, C.K. and Chang, S.W. (2008), "Atomistic simulation and investigation of nanoindentation, contact pressure and nanohardness", *Interact. Multiscale Mech.*, **1**(4), 411-422.
- Espanol, P. and Warren, P.B. (1995), "Statistical mechanics of dissipative particle dynamics", *Europhys. Lett.*, **30**(4), 191.
- Frenkel, D. and Smit, B. (2002), *Understanding molecular simulation: from algorithms to applications*, Academic Press, San Diego, USA.
- Groot, R.D. and Warren, P.B. (1997), "Dissipative particle dynamics: Bridging the gap between atomistic and mesoscopic simulation", *J. Chem. Phys.*, **107**(11), 4423.
- He, B., Patankar, N.A. and Lee, L. (2003), "Multiple equilibrium droplet shapes and design criterion for rough hydrophobic surfaces", *Langmuir*, **19**(12), 4999-5003.
- Hoogerbrugge, P.J. and Koelman, J.M.V.A. (1992), "Simulating microscopic hydrodynamic phenomena with dissipative particle dynamics", *Europhys. Lett.*, **19**(3), 155.
- Jones, J.L., Lal, M., Ruddock, J.N. and Spensley, N.A. (1999), "Dynamics of a drop at a liquid/solid interface in simple shear fields: a mesoscopic simulation study", *Faraday Discuss.*, **112**, 129-142.
- Lorensen, W.E. and Cline, H.E. (1987), "Marching cubes: A high resolution 3D surface construction algorithm", *Comput. Graph.*, **21**(4), 163-169.
- Warren, B.B. (2003), "Vapor-liquid coexistence in many-body dissipative particle dynamics", *Phys. Rev. E*, **68**(8), 066702.
- Zhao, H. and Aluru, N.R. (2008), "Molecular dynamics simulation of bulk silicon under strain", *Interact. Multiscale Mech.*, **1**(2), 303-315.